RESEARCH ARTICLE | AUGUST 19 2024

All-in-one probe for exploring self-organized two-fluid equilibria in toroidal plasmas

Special Collection: Proceedings of the 25th Topical Conference on High-Temperature Plasma Diagnostics

H. Himura ; A. F. Almagri ; J. S. Sarff ; Y. Ashida ; S. Inagaki ; H. Fujiwara ; T. Inoue ; A. Sanpei ; J. von der Linden ; K. J. McCollam ; N. C. Hurst ; C. B. Forest

Rev. Sci. Instrum. 95, 083537 (2024)
https://doi.org/10.1063/5.0215750

Review of Scientific Instruments ARTICLE pubs.aip.org/aip/rsi

All-in-one probe for exploring self-organized two-fluid equilibria in toroidal plasmas

Cite as: Rev. Sci. Instrum. 95, 083537 (2024); doi: 10.1063/5.0215750
Submitted: 25 April 2024 • Accepted: 30 July 2024 •
Published Online: 19 August 2024

H. Himura,[1,a)] A. F. Almagri,[2] J. S. Sarff,[2] Y. Ashida,[1] S. Inagaki,[1] H. Fujiwara,[1] T. Inoue,[1] A. Sanpei,[1] J. von der Linden,[3] K. J. McCollam,[2] N. C. Hurst,[2] and C. B. Forest[2]

AFFILIATIONS

[1] Department of Electronics, Kyoto Institute of Technology, Matsugasaki, Sakyo Ward, Kyoto 606-8585, Japan
[2] Department of Physics, University of Wisconsin, Madison, Wisconsin 53706, USA
[3] Max-Planck-Institute für Plasmaphysik, 85748 Garching, Germany

Note: This paper is part of the Special Topic on Proceedings of the 25th Topical Conference on High-Temperature Plasma Diagnostics.
[a)] **Author to whom correspondence should be addressed:** himura@kit.ac.jp

ABSTRACT

This paper presents the development of an all-in-one probe to simultaneously measure all components of the generalized Ohm's law in reversed-field pinch plasmas and tokamaks. The polyhedral configuration of the Mach probe is achieved through the specific arrangement, angle, and depth of the collimator channel apertures drilled into the surface of a hollow boron nitride cylinder encasing it. This probe includes a central Mach probe to assess the ion velocity field in three dimensions. Initial tests at the RELAX and Madison Symmetric Torus machines have confirmed the probe's effectiveness, revealing an octahedron form similar to a tetrahedron. The probe seems to function correctly and is expected to facilitate the empirical validation of two-fluid equilibria at the periphery of toroidal plasmas.

I. INTRODUCTION

Conventional models, such as magnetohydrodynamics (MHD), often prove inadequate in addressing dynamic research domains, such as the tokamak edge. In traditional MHD,[1] the mean velocity of the plasma flow is typically dictated by the ion fluid's velocity within the plasma. The electron fluid is implicitly regarded as the background within this framework, ensuring the plasma's charge neutrality. However, recent studies on plasma velocity have suggested the potential for decoupling ion and electron fluids in toroidal plasmas[2] and electrically non-neutral plasmas.[3] Empirical measurements of three-dimensional (3D) plasma velocity[4,5] have demonstrated such decoupling even in reversed-field pinch (RFP) plasmas, a category of magnetized toroidal plasmas. For instance, observations in RFP plasmas with plasma densities around 10^{12} cm^{-3} have indicated that the ion inertial length $\lambda_i (= c/\omega_{pi})$, also known as the ion skin depth, for hydrogen plasmas is approximately 1 cm that is a scale comparable to that of the plasma.[6] Given that λ_i represents the length scale at which the disparity in species inertia becomes significant, the findings[5] imply the existence of a two-fluid plasma state in RFP plasmas. This observation, grounded in the two-fluid plasma model,[7,8] has been extensively utilized in simulations aimed at elucidating the tokamak edge,[9] mainly due to the lower plasma density surrounding the tokamak core. Experimental investigations are imperative, as two-fluid equilibria may be significant at tokamak edges and in RFP plasmas characterized by low plasma densities.

The most straightforward way for testing two-fluid descriptions shown in Fig. 1 is to simultaneously measure all the terms included in Ohm's law for a magnetized plasma[10] by using internal probes, especially the $\vec{u}_i \times \vec{B}$ and the Hall ($\propto \vec{J} \times \vec{B}$) terms,

$$\vec{E} = -\vec{u}_i \times \vec{B} + \frac{d_i}{n}(\vec{J} \times \vec{B} - \nabla p_e) + \frac{{d_e}^2}{n}\frac{d\vec{J}}{dt} + \eta\vec{J} - \eta_2 {\nabla_\perp}^2 \vec{J}, \quad (1)$$

where d_i and d_e are the ratios of λ_i and the electron skin depth $\lambda_e (= c/\omega_{pe})$ to a typical scale length L in the plasma, respectively.

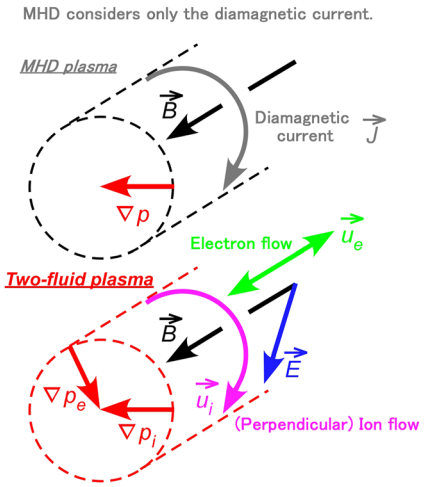

FIG. 1. Comparison of the two-fluid plasma with an MHD. Many vector terms, especially the ion fluid velocity field, appear in the two-fluid plasma.

In addition, $\vec{E}$, $\vec{u}_i$, $\vec{B}$, $\vec{J}$, and p_e are the electric, ion velocity, magnetic fields, plasma current, and electron pressure, respectively. Both η and η_2 are called resistivity and hyper-resistivity, respectively.[10,11] This experimental test can be conducted by active probing in medium-sized toroidal machines such as MST and RELAX[12] constructed initially to operate as RFPs. Recently, these machines have been used to investigate ohmically heated circular cross-sectional tokamaks. Comparative analyses between circular cross-section tokamaks and RFPs within the same apparatus have revealed a parameter range in the low $q(a)$ region,[13] where q represents the safety factor and a denotes the minor radius of a toroidal plasma. Furthermore, such devices can subtly adjust the q profile within a range that stretches from positive $q(a)$ values characteristic of tokamak-like and ultra-low q configurations to negative $q(a)$ values indicative of RFP configurations within the same apparatus.[12] Figure 2 shows typical q profiles[12] of a tokamak and an RFP. In the tokamak case, the value of $q(r)$ at the plasma center ($r = 0$) exceeds unity and gradually increases to approximately three at the plasma edge ($r/a = 1$). In contrast, $q(r)$ at the plasma center is less than unity for the RFP scenario and gradually decreases to approximately −0.5. This feature indicates the potential for a $q = 0$ magnetic surface, across which the toroidal magnetic field direction (B_t) becomes antiparallel in RFP plasmas.

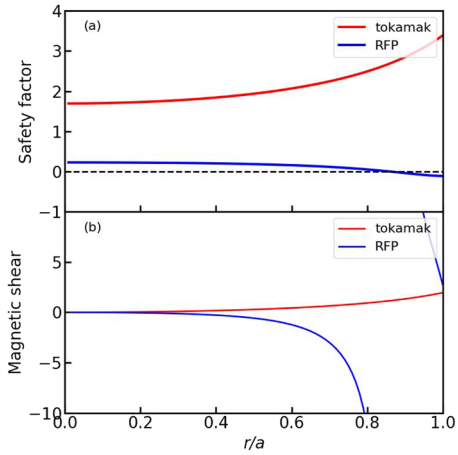

FIG. 2. Typical radial profiles of (a) the safety factor q and (b) the magnetic shear s of RFP, ultra-low-q, and tokamak plasmas.

The distinction mentioned above enables systematic examinations of the dependence of two-fluid states on the q profile or magnetic shear s within the same apparatus, where s is defined as $s \equiv (a/q(r))q'(r)$. In particular, $s(r)$ diverges entirely in the RFPs due to the presence of the $q = 0$ surface. Figure 2 also shows typical s profiles of an RFP and a tokamak. The divergence of $s(r)$ occurs around $r/a \sim 0.8$ in the RFP, while no such separation occurs in the tokamak. Another notable distinction in $s(r)$ is that it increases significantly throughout the RFP region compared to tokamaks. This phenomenon also allows us to explore potential correlations between $s(r)$ and two-fluid states, warranting experimental investigation in laboratory toroidal plasmas. In addition, RFP and tokamak plasmas exhibit sawtooth processes in which tearing modes appear and seem to be responsible for relaxation dynamics.[7] The sawtooth process entails significant and rapid changes in the generalized Ohm's law, making it an excellent experimental test bed for assessing the role of various terms. For these reasons, the RELAX machine has initiated the form of tokamak plasmas[12] and RFPs to investigate the validity of the two-fluid state experimentally. However, several limitations remain in RELAX. First, plasma currents I_p are ~50 kA for RFP and ten kA for tokamaks. Those values are lower than those in MST, indicating that RELAX is collisional compared to MST. Second, the flat-top time of I_p is in millisecond order, in contrast to the tens of milliseconds in MST. Therefore, to systematically test two-fluid equilibrium, we conducted parallel experiments with a novel probe at MST and RELAX as a collaborative study of the two-fluid state in magnetized toroidal plasmas.

II. ALL-IN-ONE PROBE

Figure 3 shows a schematic of the new all-in-one probe to measure the three-dimensional vector quantities of magnetic $\vec{B}$, electric $\vec{E}$, and ion fluid velocity $\vec{u}_i$ fields.

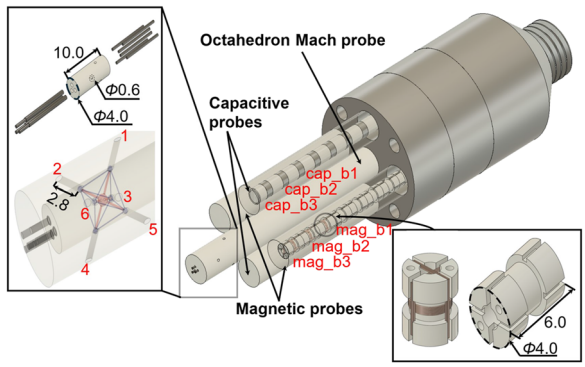

FIG. 3. Schematic of the all-in-one probe we proposed, which consists of five fingers. The central finger contains an octahedron-type Mach probe and a triple probe. The other two fingers are employed for magnetic probe arrays, and the other two are for capacitive probe arrays.

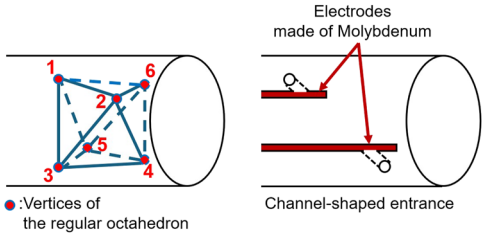

FIG. 4. Schematic of the octahedron-shaped Mach probe. All the electrodes for the probe use six straight rods made of molybdenum. The six holes on the surface of the rod made of boron nitride make the octahedron-shaped collectors for ion saturation currents.

The central finger contains a polyhedron-shaped Mach probe.[14] The distance between adjacent octahedral collectors is 5.66 mm, while 8.0 mm between the diagonal collectors. These distances are approximately equal to or less than the theoretically predicted spatial scale length for a two-fluid state, i.e., λ_i. To position the collectors at the apexes of the octahedron, a set of collimator channels, oriented in a specific direction, as shown in Fig. 4, is drilled on the surface of the cylindrical rod made of boron Nntride (BN). This paper proposes this unique feature. Unlike conventional placement at each vertex of the octahedron, collectors are strictly oriented so that the set of collimator channels in the BN cylindrical rod only measures the ion saturation currents I_{sat} flowing into each vertex, as recognized from a schematic drawing to assembly the Mach probe shown in Fig. 5. This method simplifies the fabrication of polyhedral Mach probes and has been successfully applied to tetrahedral Mach probes in the RELAX machine.

For the prototype all-in-one probe shown in Fig. 3, the channel pore depth is set at ~1 mm. Since $|\vec{B}| \sim 500$ G in MST and RELAX, the gyroradius ($\equiv m_i v_\perp/(q|\vec{B}|)$) of the ions in hydrogen plasmas reads $\sim 2.8\sqrt{T_i[\mathrm{eV}]}$ (mm). Thus, $T_i \ll 10$ eV should yield an accurate $|\vec{u}_i|$. This result can be called a probe measurement for a strongly magnetized plasma. On the other hand, when $T_i \sim 10$ eV, the current due to the gyro motion is mixed into I_{sat}. This uncertainty can be termed a probe measurement for a weakly magnetized plasma.[15] In this case, we must pay attention to the value of I_{sat}, which should be excessive.

Regarding Mach number M_α where $\alpha = \{x, y, z\}$, we plan to determine the 3D plasma velocity from the six I_{sat} values obtained from the octahedron-shaped Mach probe.

The radial profile of M_α is obtained by moving the all-in-one probe in the radial direction. Once M_α is obtained, $\vec{u_i}$ is calculated as $u_{i\alpha} = M_\alpha C_s$ using the formula of $C_s = \sqrt{(\gamma\kappa T_i + Z\kappa T_e)/m_i}$, where γ, κ, and Z are the adiabatic coefficient, Boltzmann's constant, and the ionization number, respectively. The triple probe attached to the top of the central finger measures the electron temperature T_e ($\approx T_i$) required for this calculation at each measurement point. Similarly, the radial profiles of the electron density n_e can be obtained by moving the all-in-one probe radially. Based on these measurements, $\vec{u_i}(r)$ is determined. Only the central finger is longer than the other four fingers to ensure the other four fingers do not obstruct the I_{sat} flowing into this octahedron-shaped Mach probe.

The return electrode for sending all I_{sat} back to the plasma is a single-pin electrode positioned adjacent to the three-pin electrodes used for the triple probe. This single-pin electrode returns six I_{sat} currents to the plasma for the octahedron case. Figure 6 shows this circuit configuration. The negative voltage applied to the Mach electrodes is set with respect to the plasma floating potential of the return electrode (also see Fig. 6). The negative bias voltage up to −200 V, approximately $(3 \sim 4) \times T_e$, is planned to apply to the six molybdenum rods.

The dimensions of the pickup coil to measure B_x ($= B_p$) are 4.0, 5.4, and 0.8 mm in length, width, and height, respectively. Similarly, those measuring B_y ($= B_t$) are 4.0, 6.6, and 0.8 mm in length, width, and height, respectively. For measuring B_z ($= B_r$), the diameter is 4.8 mm and the height is 5.0 mm. Enameled wires with a diameter of 0.2 mm are wound around pickup coils for B_x and B_y with six turns, while 50 turns for B_z. Six pickup coils are aligned on each of the two fingers with an interval of 9.0 mm. These measure the magnitudes of B_t, B_p, and B_r. The spatial gradient values of B_t, B_p, and B_r are also measured by rotating the symmetry axis of the all-in-one probe.

The remaining two of the five fingers serve as capacitive probes.[16] Within each capacitive probe, rings made of SUS304 with an inner diameter of 5.0 mm, an outer diameter of 6.9 mm, and a height of 2.0 mm are positioned at intervals of 4.5 mm. The hollow cylinder that covers these rings is also made of BN, allowing the space potential to be determined by the emission of thermal electrons from BN if $T_e >\sim 30$ eV. The component E_p or E_t of $\vec{E}$ can be

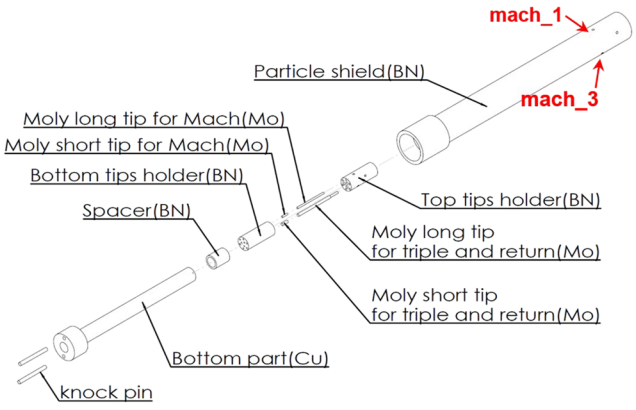

FIG. 5. Schematic of the assembly of the octahedron-shaped Mach probe.

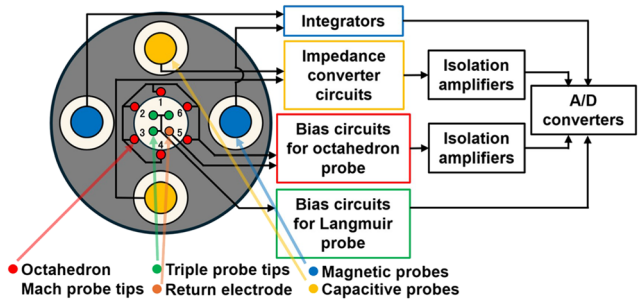

FIG. 6. Schematic of the circuit diagram of the all-in-one probe.

obtained by rotating the all-in-one probe. The E_r component of $\vec{E}$ is obtained in one attempt.

We originally built an isolation amplifier with a flat-top frequency response up to a 1 MHz bandwidth for the presented experiment. However, during the initial experiment conducted in MST, which will be detailed later, we opted not to use the 1 MHz bandwidth isolation amplifier. The difference in the reference potential of the Mach probe between RELAX and MST influenced this decision. The reference potential of the Mach probe is the plasma floating potential in RELAX. On the other hand, it was the vacuum wall, which was COM, in MST. For the measurements presented with the all-in-one probe, the position of COM was finally changed to three plasma floating Mach tips near the other three collector tips. We will come back again to this point. As a result, the isolation amplifiers used in the first series of the MST experiment had a flat-top bandwidth of up to several 100 kHz. It is important to note that this limited their reliability for frequency components above ~100 kHz in the measured signal.

III. PRELIMINARY RESULT AND DISCUSSION

Initial experiments with the tetrahedral (not presented in this paper) and octahedral configurations of the all-in-one probe, featuring polyhedral Mach probes, were conducted on RELAX and MST machines, respectively. As shown in Fig. 7, during the MST experiment, the all-in-one probe was vertically inserted downward along the MST's symmetry axis from port No. 155 on the top side of the machine. The probe comprises a total of 44 signal channels. The prototype all-in-one probe utilized hermetically sealed multichannel current terminals, transmitting all the signals by connecting two current terminals to a T-shaped tube.

Plasmas formed in the MST device exhibit characteristics of both RFP and tokamak configurations. The all-in-one probe moved within the edge region of each plasma, up to 10 cm from the inner wall of the MST. Figure 8 shows the plasma current I_p, the loop voltage V_{loop}, the plasma edge toroidal magnetic field B_t, its plasma cross-sectional average $\langle B_t \rangle$, and the time variation of the line-averaged electron density n_e. In particular, the maximum value of I_p is ~200 kA, with a flat-top duration of about 0.02 s. Repeated events indicative of sawtooth instability are observable in V_{loop}, $\langle B_t \rangle$, and B_t. Furthermore, the negative value of B_t signifies the RFP nature of

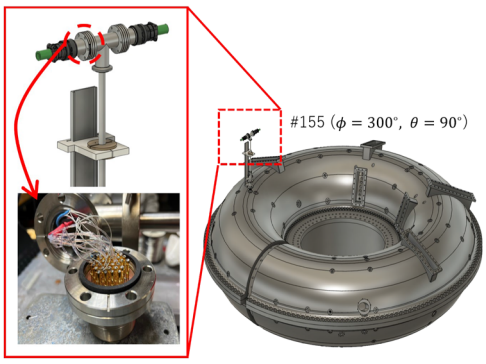

FIG. 7. Schematic of the setup of the all-in-one probe on the MST machine.

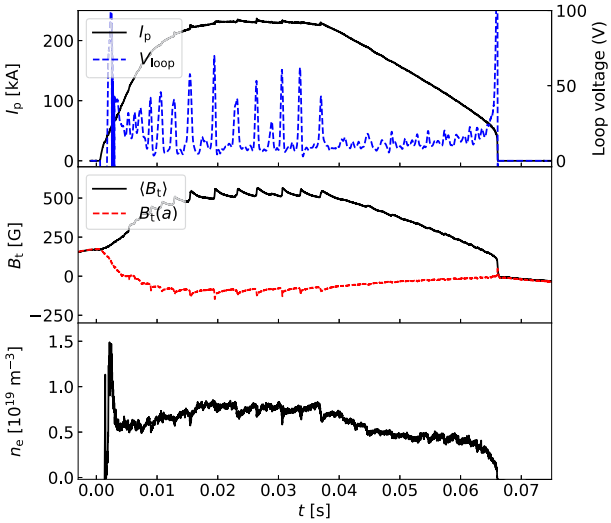

FIG. 8. Typical waveforms of the plasma current, the loop voltage, a pickup coil, and the line-averaged density of a toroidal plasma produced in MST.

the plasma. The line-averaged value of n_e is ~0.8×10^{19} m^{-3}. When MST forms a tokamak, the maximum of I_p was about 50 kA and the value of B_t became positive. Operating at this lower I_p has the advantage of reducing the load on the all-in-one probe, leading to an extended probe lifetime. Consequently, and given the unexplored nature of two-fluid studies at MST, the all-in-one probe was utilized for the edge plasmas.

Figure 9 shows representative datasets for the components B_t and B_r of $\vec{B}$, which were recorded at the periphery of the RFP using the all-in-one probe. In addition, it includes the plasma potential

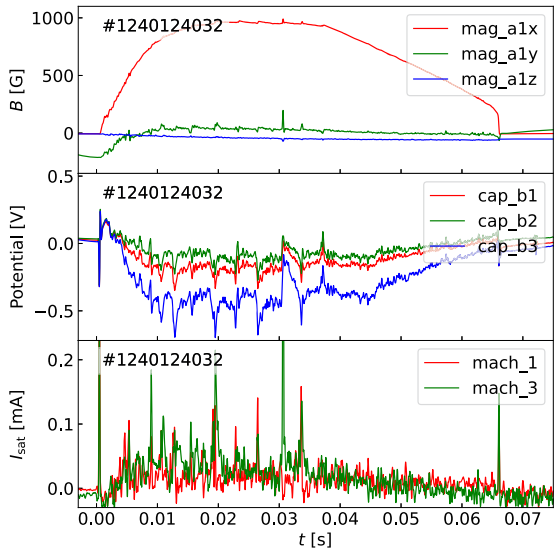

FIG. 9. All-in-one probe measures typical data of probe signals.

at three distinct measurement locations and the temporal variation of I_{sat} entering the two apexes of the octahedron. Throughout this experimental series, we employed the remaining three Mach tips, specifically tips 2, 4, and 6, as return electrodes (also see Figs. 4 and 6). A notable $B_x(=B_p)$ component is detected in the RFP plasma configuration, characterized by a distinct flat top. On the other hand, the B_r component is approximately zero. The capacitive probe signals exhibit a similar increase in the pickup coil signal. The differing values at three separate measurement points indicate the presence of E_r. The numerous spikes in all signals may indicate a plasma macroscopic mode, such as a locked one and relaxation events. Empirically, when such an event occurs, a backflow of fast electrons from the wall made of aluminum seems to generate, which might have entered Mach tips.

Several fluctuations are also detected with respect to I_{sat} emanating from the octahedron-shaped Mach probe. The mean output of I_{sat} is around 30 μA. Based on these individual readings, we infer that the all-in-one probe mainly operates correctly. With a surface area of ≈0.28 mm^{-2}, the particle flux nv is estimated to be $\sim 7 \times 10^{20}/\mathrm{m}^2\mathrm{s}$. Although the local value of n remains undetermined due to the malfunction of the triple probe during this initial experiment, we estimate that v is $\sim 10^2$ m/s using the standard value of 0.8×10^{19} m^{-3} for n in the plasma center, as measured by the interferometer. The substituted n_e in the plasma core as n suggests that the derived v represents a lower bound of $|\vec{u}_i|$. Therefore, the next question is whether Mach numbers indicating velocities above this lower limit can be accurately measured using polyhedral probes. In fact, empirical data obtained using a tetrahedral probe in RELAX-RFP plasmas have shown values that indicate the Mach number in the poloidal direction of approximately unity. This implies that the typical speed in the poloidal direction is around 1 km/s. However, these results need further confirmation, which will be reported elsewhere. Upcoming experiments, which will record signals from all octahedron channels, will further investigate and confirm the effectiveness of the all-in-one probe in empirically studying two-fluid equilibria at the edge of toroidal plasmas.

Finally, we briefly refer to the RELAX-RFP and MST-tokamak experiments, which were omitted because of space constraints. Substantial I_{sat} readings were acquired from the four Mach tip electrodes in the RELAX-RFP experiment. However, in the MST-tokamak experiment, the all-in-one probe exhibited a low signal-to-noise ratio due to excessive switching noise from the power supply during plasma generation. Consequently, the next experiment will employ an all-in-one probe with improved shielding.

IV. SUMMARY

This investigation delineates the development of an all-in-one probe designed to examine two-fluid plasmas in the peripheral regions of RFPs and tokamaks. The all-in-one probe comprises a central polyhedral Mach probe surrounded by magnetic, capacitive, and triple probes. The polyhedral configuration of the Mach probe is achieved through the specific arrangement, angular orientation, and depth of the collimator channel apertures drilled into the surface of a hollow BN cylinder that houses it. Preliminary trials conducted at RELAX with tetrahedral Mach tips (not included in this paper) and at MST with octahedral Mach tips have predominantly validated the functional efficacy of the magnetic, capacitive, and Mach probes within the all-in-one probe, except the triple probe. Subsequent efforts will enhance the all-in-one probe by incorporating the octahedral Mach probe into a more resilient version capable of simultaneously capturing signals from all 44 channels. These comprehensive measurements will facilitate the empirical validation of the generalized Ohm's law in the low-density plasma edge region, characterized by an extended ion skin depth.

ACKNOWLEDGMENTS

The authors thank Mr. R. Takaoka for his initial work on the prototype all-in-one probe, Mr. T. Sasaki for his assistance with the RELAX machine, and Mr. P Wilhite for data conversion. This work was supported by JSPS KAKENHI Grant No. 23KK0053. This material is based upon the work supported by the U.S. Department of Energy, Office of Science, Office of Fusion Energy Sciences under Award No. DE-SC0018266 for the Wisconsin Plasma Physics Laboratory (WiPPL).

AUTHOR DECLARATIONS

Conflict of Interest

The authors have no conflicts to disclose.

Author Contributions

H. Himura: Conceptualization (lead); Funding acquisition (lead); Investigation (lead); Methodology (lead); Writing – original draft (lead); Writing – review & editing (lead). **A. F. Almagri**: Conceptualization (equal); Investigation (equal); Methodology (equal). **J. S. Sarff**: Investigation (equal); Supervision (lead). **Y. Ashida**: Data curation (equal); Investigation (supporting); Methodology (supporting). **S. Inagaki**: Investigation (supporting); Visualization (lead). **H. Fujiwara**: Investigation (supporting). **T. Inoue**: Investigation (supporting). **A. Sanpei**: Data curation (lead); Software (lead). **J. von der Linden**: Supervision (supporting). **K. J. McCollam**: Formal analysis (lead). **N. C. Hurst**: Investigation (supporting). **C. B. Forest**: Project administration (lead).

DATA AVAILABILITY

The data support the findings of this study are available from the corresponding author upon reasonable request.

REFERENCES

[1] Y. Peng, Y. Yang, Y. Jia, B. Rao, M. Zhang, Z. Wang, H. Wang, and Y. Pan, Nucl. Fusion **62**, 066037 (2022).
[2] N. Hurst and J. Sarff, Private Communications (2022).
[3] Y. Nakajima, H. Himura, and A. Sanpei, J. Plasma Phys. **87**, 905870415 (2021).
[4] D. J. Den Hartog, J. Chapman, D. Craig, G. Fiksel, P. Fontana, S. Prager, and J. Sarff, Phys. Plasmas **6**, 1813 (1999).
[5] J. Boguski, M. Nornberg, U. Gupta, K. McCollam, A. Almagri, B. Chapman, D. Craig, T. Nishizawa, J. Sarff, C. Sovinec, P. Terry, and Z. Xing, Phys. Plasmas **28**, 012510 (2021).
[6] S. Kawai, H. Himura, S. Masamune, and J. Aoki, Phys. Plasmas **23**, 022113 (2016).

[7]L. Marrelli, P. Martin, M. Puiatti, J. Sarff, B. Chapman, J. Drake, D. Escande, and S. Masamune, Nucl. Fusion **61**, 023001 (2021).
[8]C. Sovinec, J. King, and NIMROD Team, J. Comput. Phys. **229**, 5803 (2010).
[9]B. Zhu, M. Francisquez, and B. Rogers, Comput. Phys. Commun. **232**, 46 (2018).
[10]D. Biskamp, *Magnetic Reconnection in Plasmas* (2000), p. 204.
[11]H. Strauss, Phys. Fluids **29**, 3668 (1986).
[12]T. Inoue, H. Himura, A. Sanpei, T. Murase, S. Nakagawa, T. Shimizu, A. Shimizu, M. Isobe, and H. Hayashi, Fusion Eng. Des. **184**, 113285 (2022).
[13]N. Hurst, B. Chapman, A. Almagri, B. Cornille, S. Kubala, K. McCollam, J. Sarff, C. Sovinec, J. Anderson, D. Den Hartog, C. Forest, M. Pandya, and W. Solsrud, Phys. Plasmas **29**, 080704 (2022).
[14]A. Sellner, J. von der Linden, H. Himura, R. Reksoatmodjo, J. Sears, S. You, A. Almagri, K. McCollam, M. Reyfman, C. Rouda, and J. Sarff, Rev. Sci. Instrum. **95**, 073536 (2024) accepted for publication in.
[15]H. Himura, C. Nakashima, H. Saito, and Z. Yoshida, Phys. Plasmas **8**, 4651 (2001).
[16]T. Nishizawa, A. Almagri, W. Goodman, S. Ohshima, and J. Sarff, Rev. Sci. Instrum. **89**, 10J118 (2018).